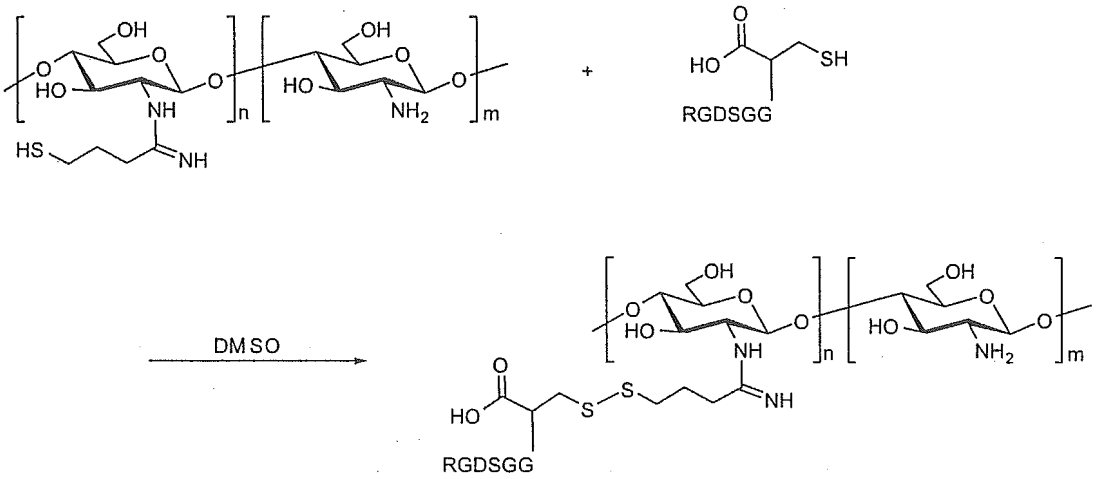

Scheme 3. Coupling reaction of SH-chitosan with RGDSGGC in the presence of DMSO.

2.5. Cell adhesion assay

Cell adhesion assay was performed essentially according to the method described previously [35,36]. In brief, wells of 96-well microtiter plates (Nunc-Immuno^{TM} Plates, NUNC, Rochester, NY, USA) were coated with 50 μl of the RGDSGGC–chitosan solution to each well and incubated at 37 °C for 1 h in a 5% CO_2 incubator. Three kinds of plates were prepared in accordance with the concentration of the material and were termed as 0.12% hybrid, 0.012% hybrid, and 0.0012% hybrid. In addition, 0.00185% RGDSGGC solution, which is equivalent to the amount of RGDSGGC in 0.12% hybrid, was also used for coating the plate (in the text, this plate was called as "non-hybrid"). As a control, non-coating wells were prepared. Nonspecific binding sites were blocked by incubating the plates with 100 μl of 1% bovine serum albumin for 1 h at room temperature. The wells were then washed three times with PBS. Chondrocytes and fibroblasts (1×10^5 cells/well) in 100 μl of HEPES buffer were added to the wells and incubated for 1 h at 37 °C. After the removal of the unbound cells by gently rinsing the wells three times with PBS, the cells attached to the 96-well plates were added 50 μl of 0.25% crystal violet (WAKO Pure Chemicals Co. Ltd., Osaka, Japan) in 20% methanol and incubated for 30 min at room temperature. After rinsing by distilled water, 100 μl/well of 20% acetic acid was added. The degree of cell adhesion was quantified with an optical density at 590 nm by Microplate Reader Model 550 (Bio-Rad, Hercules, CA, USA).

2.6. Cell proliferation assay

Cell proliferation assay was performed by 2-(2-methoxy-4-nitrophenyl)-3-(4-nitrophenyl)-5-(2, 4-disulfophenyl)-2H-tetrazolium, monosodium salt (WST-8) procedures basically as previously described [37,38]. 1-methoxy-5-methylphenazinium methosulfate (1-Methoxy PMS) and other reagents were obtained from Dojindo Laboratories (Kumamoto, Japan). 96-well microtiter plates (Nunc MicroWell^{TM} Plates, NUNC, Rochester, NY, USA) were coated with 50 μl of RGDSGGC–chitosan conjugate solutions in a similar manner as described in the section of cell adhesion assay. As controls, non-coating plate (Control 1) and 0.12% SH-chitosan-coated plate [chitosan-2-iminothiolane complex, the intermediate without RGDSGGC (Control 2)] were also prepared. Non-specific binding sites were blocked by incubating the plates with 100 μl/well of 1% bovine serum albumin for 1 h at room temperature. The wells were then washed three times with PBS. Chondrocytes (100 μl, 2.25×10^5 cells/ml) suspension was added to the wells and incubated at 37 °C for 24 h. Fibroblasts (100 μl, 2.6×10^5 cells/ml) suspension was added to the wells and incubated for 24 h at 37 °C. A 10 μl of the working solution containing WST-8 and 1-Methoxy PMS (0.5 mM and 20 μM, respectively, as the final concentration) was added to each well. Then, the mixtures were incubated for an additional 2 h. The absorbance of each well was measured at 490 nm by using Microplate Reader Model 550 (Bio-Rad, Hercules, CA, USA). Statistical analyses were performed by using variance (ANOVA) and with Fisher's protected least significant difference post hoc test. Differences were considered significant for $p < 0.05$.

3. Results and discussion

3.1. Preparation of chitosan–RGDSGGC conjugate

It has been known that 2-iminothiolane reacts with general primary amines including N-terminal α-and

ε-amino groups of peptides or proteins by a ring-opening reaction [30]. As a result, a reactive sulfhydryl group attached through the linker moiety with an appropriate distance from peptide main chain could be generated as a potential cross-linking group in the proteins [30–33]. However, this useful method has not been applied for the preparation of polysaccharide derivatives yet. The reaction of 2-iminothiolane with chitosan in proceeded smoothly in an acidic aqueous solution and finally gave a clear solution of the neutral or alkaline condition. The merit of this much improved solubility of novel SH-chitosan is evident because subsequent coupling reaction with peptides or proteins can be carried out under a mild and homogeneous solution. As expected, the amino acid analysis of the product (Fig. 2) revealed the high efficiency in the coupling reaction of RGDSGGC with SH-chitosan in the presence of DMSO as an oxidation reagent [34]. The degree of substitution (DS) of the peptide on SH-chitosan was estimated to be DS = 0.25. Although extensive efforts had been paid toward derivatization of chitosan in terms of the development of bio-related materials, they usually require tedious and time-consuming processes for chemical modifications in the general organic solvents [39]. Chitin derivative bearing sulfhydryl groups at C-6 position (SH-chitin) was also prepared as an intermediate for the synthesis of graft copolymers such as chitin/polystyrene hybrid materials [40]. However, these derivatives usually show extremely poor solubility to water and aqueous buffer solutions. Considering the feasibility to the preparation of a variety of hybrid-type materials in tissue engineering, water soluble SH-chitosan prepared on the basis of 2-iminothiolane will become a key versatile intermediate both for conjugating bioactive components and for coating (hybridizing) with other substances. In addition, we have already reported that polyion complex (PIC) fibers based on chitosan-alginate hybrid showed an excellent property for scaffolds in cartilage tissue engineering [41]. These results clearly suggest high potentials and wide applicability of 2-iminothiolane-based conjugation strategy of chitosan with biologically important substances.

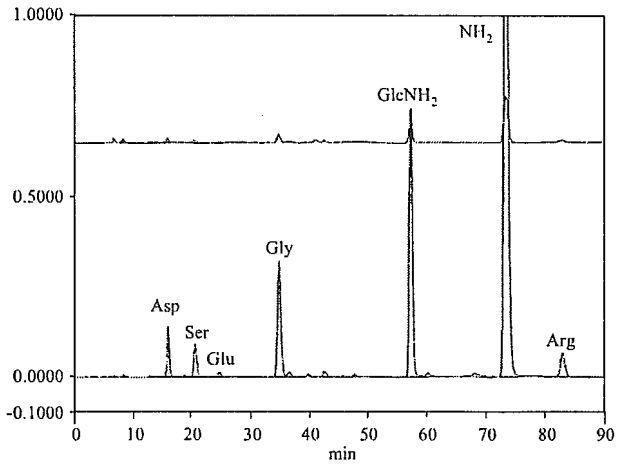

Fig. 2. Amino acid analysis of the hydrolysate of chitosan–RGDSGGC conjugate.

3.2. Cell adhesion assay

Fig. 3 shows phase-contrast microscopic pictures of chondrocytes adhering on plates. It was clearly observed that chondrocytes adhered preferentially onto the plate coated with chitosan–RGDSGGC (Fig. 3A, 0.12% hybrid) in comparison with the plate coated with RGDSGGC (Fig. 3B, non-hybrid). As shown in Fig. 4, the plates coated with 0.12% hybrid had the highest adhesivity of chondrocytes among all plates. Similarly, fibroblasts also adhered onto the plates coated with chitosan–RGDSGGC conjugate in proportion to the amount of the hybrid scaffold employed (Fig. 5). These results suggest that introduction of RGDSGGC moiety to SH-chitosan markedly enhanced affinity both of chondrocytes and fibroblasts with this polysaccharide scaffold.

3.3. Cell proliferation assay

Next, we examined the effect of the introduction of the cell adhesive peptide to chitosan on the cell shape

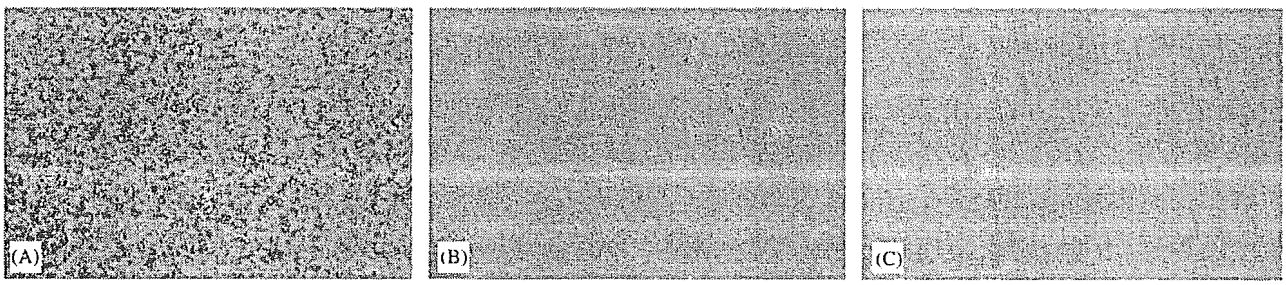

Fig. 3. Pictures of phase-contrast microscope showing chondrocytes adhering to the plates coated with (A) 0.12% hybrid (chitosan–RGDSGGC), (B) non-hybrid (RGDSGGC) and (C) control (original magnification × 40).

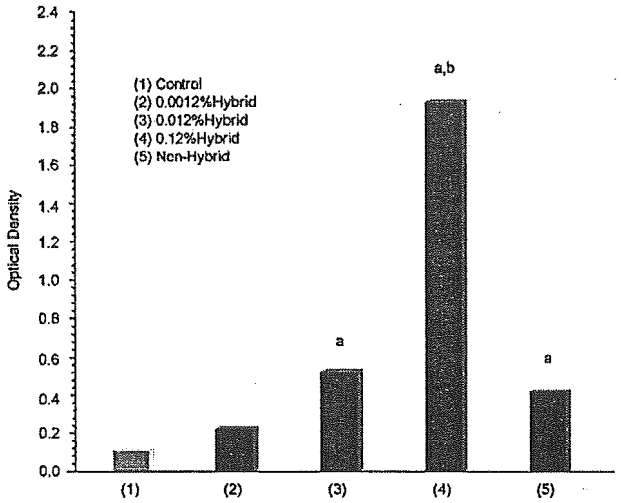

Fig. 4. Chondrocyte cell adhesivity. Chitosan–RGDSGGC conjugates (0.12% and 0.012% hybrid) and non-hybrid showed significant cell adhesion capacities to chondrocytes ($^{a}p<0.0001$ vs. control). 0.12% hybrid exhibited the highest adhesivity with chondrocytes. 0.12% hybrid also showed significant cell adhesion capacity compared with non-hybrid ($^{b}p<0.0001$ vs. non-hybrid).

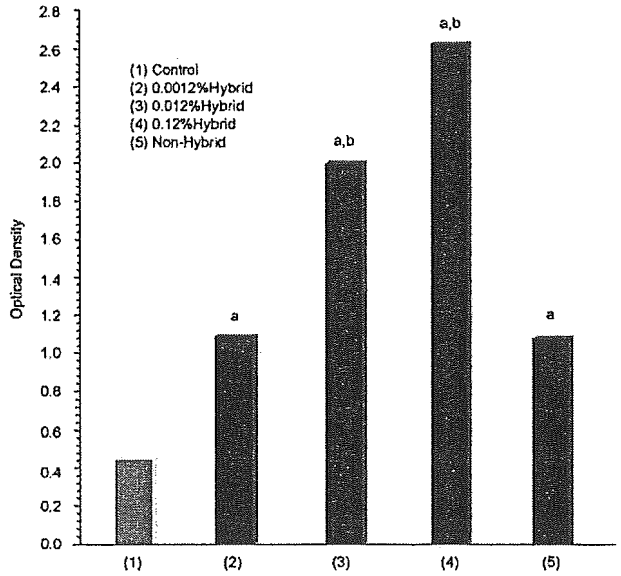

Fig. 5. Fibroblast cell adhesivity. All chitosan–RGDSGGC conjugates and non-hybrid showed significant cell adhesion capacities to fibroblasts ($^{a}p<0.0001$ vs. control). Two chitosan–RGDSGGC conjugates (0.12% hybrid and 0.012% hybrid) exhibited much higher adhesivities with fibroblasts than non-hybrid ($^{b}p<0.0001$ vs. non-hybrid).

change in terms of the characterization of the suitability as a scaffold material having potentials for inducing cell proliferation on the plates. As shown in Fig. 6, chitosan–RGDSGGC conjugate (Fig. 6A, 0.012% hybrid) also exhibited much improved cell proliferation

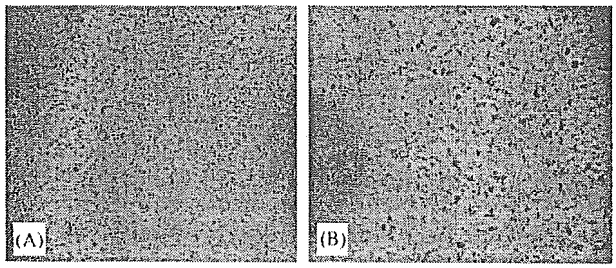

Fig. 6. Pictures of phase-contrast microscope showing chondrocytes proliferation on the plates coating with (A) 0.012% hybrid and (B) non-hybrid (RGDSGGC) (original magnification ×40).

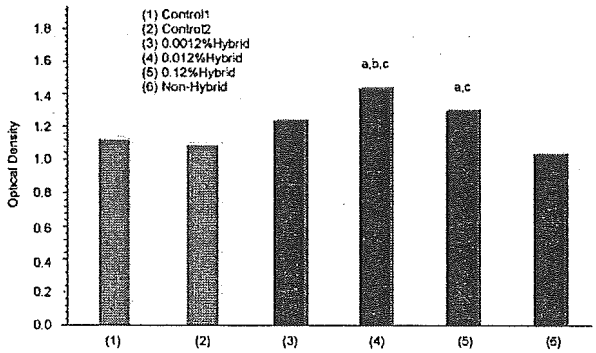

Fig. 7. Chondrocyte cell proliferation activity. Chitosan–RGDSGGC conjugates (0.12% hybrid and 0.012% hybrid) showed higher cell proliferation activities than Control 1 and Control 2 ($^{a}p<0.001$ vs. Control 1 and $^{c}p<0.001$ vs. Control 2), respectively. These results indicated that 0.012% hybrid had the most effective cell proliferation activity to chondrocytes ($^{b}p<0.02$ vs. others).

activity of chondrocytes compared with RGDSGGC (Fig. 6B, non-hybrid). Adhered chondrocytes on the plate coated with 0.012% hybrid significantly induced their shape change, while the plate coated with non-hybrid showed little effect on the cell proliferation activity to adhered chondrocytes. Cell proliferation activities of the novel chitosan derivatives were evaluated by using chondrocytes and fibroblasts as shown in Figs. 7 and 8. It was suggested that the introduction of RGDSGGC component to chitosan significantly enhanced chondrocyte cell proliferation and the optimal effect on the cell shape change was observed in the case of the plate coated with 0.012% hybrid. There was not so meaningful difference of the chondrocytes proliferation activity among these three hybrid materials. On the other hand, fibroblast cell proliferation was enhanced in proportion to the concentration of chitosan–RGDSGGC used for the coating the plates as shown in Fig. 8.

The improved cell adhesion and proliferation activities of chitosan–RGDSGGC conjugate seem to be greatly dependent on the integrin-mediated signal transduction. Integrins have been well known to bind

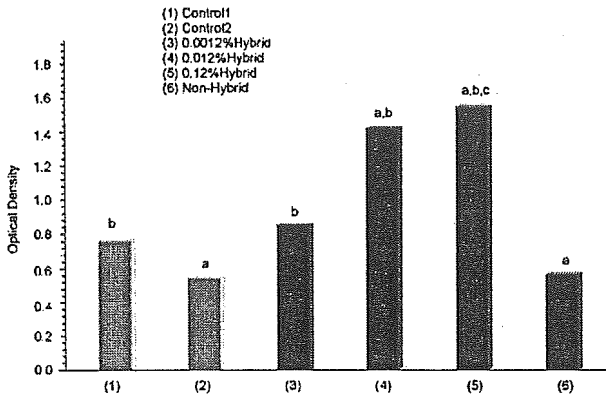

Fig. 8. Fibroblast cell proliferation activity. Chitosan–RGDSGGC conjugates (0.12% hybrid and 0.012% hybrid) showed significant cell proliferation activities, while Control 2 and non-hybrid exhibited significant anti-proliferation activities ($^{a}p<0.001$ vs. Control 1). Control 1 and all chitosan–RGDSGGC conjugates showed significant cell proliferation activities compared with Control 2 ($^{b}p<0.001$ vs. Control 2). These results indicated that 0.12% hybrid had the most effective cell proliferation activity to fibroblasts ($^{c}p<0.01$ vs. others).

a variety of cells and influence cellular functions such as cell proliferation, cell differentiation, and productions of ECM molecules. In the living body, they are involved in embryogenesis, inflammation, wound healing, and thrombosis as well as tumor invasion and metastasis [42,43]. Expression of integrin subunits α_1, α_5, α_v, β_1, β_4, and β_5, was found on the cell surface of freshly isolated human chondrocytes [44–46], while integrin subunits α_2, α_3, α_5, and β_1, were proved to be expressed on the cell surfaces of fibroblasts. Especially, fibronectin receptor $\alpha_5\beta_1$ is involved in chondrocyte and fibroblast adhesion, spreading, and proliferation on fibronectin [47], and acts as a mechanoreceptor [48,49]. These findings are consistent with our current results.

Since one of the considerable limitations is that the present study showed no in vivo data, we must perform further investigation to evaluate the biocompatibility and biodegradability in animal models. Then, the novel chitosan conjugate will be applied to the scaffold materials for the tissue regeneration experiments. The other limitation is that the current results are based on only the chondrocytes and fibroblasts. Ideally, various kinds of cells should be evaluated to clarify the effects of this novel material on the cellular functions. For instance, similar results have been observed with porcine aortic endothelial cells, where covalently attached RGD-peptides stimulated adhesion and spreading of the cells on different polymers [50]. Moreover, adhesion of several cell types (e.g. human aortic smooth muscle cells and human dermal fibroblasts) proved to be enhanced by increasing the amount of RGD-peptide coated on glass substrates. To control the signal transduction between cells and the scaffold materials, we will design and prepare new chitosan-based scaffold materials on the basis of the present 2-iminothiolane mediated conjugation strategy.

4. Conclusions

In the present study, we established a facile and efficient method for the conjugation of chitosan with SH-containing synthetic peptide on the basis of 2-iminothiolane mediated selective cross-linking under a mild and homogeneous solution. It was demonstrated that chitosan–RGDSGGC conjugate exhibited highly excellent cell adhesion and proliferation activity in chondrocytes and fibroblasts. The results obtained in this study clearly suggest that introduction of cell adhesive-small-peptide component related to the cell binding domain of fibronectin provides chitosan with much improved and desirable properties as a potent scaffold material in musculoskeletal tissue engineering. The merit of this method is evident because the flexible sulfhydryl groups attached at C-2 positions of chitosan could be applied for the modification not only by small peptides but also high-molecular-weight of proteins that regulate cell growth and/or cell differentiation as well as cell proliferation.

Acknowledgements

This research was partly funded by the Hokkaido Bureau of the Ministry of Economy, Trade and Industry and by Northern Advancement Center for Science & Technology in Hokkaido. S.-I. N. appreciates to the support from NEDO for "Research and Development on Glycocluster Controlling Biomolecules (1999–2004)". And it was also funded by Grant-in-Aid for Scientific Research from the Japan Ministry of Education, Culture, Sports, Science, & Technology (B-1539044), and Grant-in-Aid for New Energy and Industrial Technology Development Organization (03A04002a).

References

[1] Brittberg M, Lindahl A, Nilsson A, Ohlsson C, Isaksson O, Peterson L. Treatment of deep cartilage defects in the knee with autologous chondrocyte transplantation. New Engl J Med 1994;331:889–95.
[2] Bell E, Ivarsson B, Merrill C. Production of a tissue-like structure and contraction of collagen lattices by human fibloblasts of different proliferative potential in vitro. Proc Natl Acad Sci USA 1979;76:1274–8.
[3] Hansbrough JF, Christine D, Hansbrough WB. Clinical trials of a living dermal tissue replacement placed beneath meshed, splilit-thickness skin grafts on excised burn wounds. J Burn Care Rehabil 1992;13:519–29.

[4] Lundborg G, Gelberman RH, Longo FM, Dowell HC, Varon S. In vivo regeneration of cut nerves encased in silicone tubes. J Neuropathol Exp Neurol 1982;41:412–22.
[5] Langer R, Vacanty JP. Tissue engineering. Science 1993; 260:920–6.
[6] Peppas NA, Langer R. New challenges in biomaterials. Science 1994;263:1715–20.
[7] Sittinger M, Reitzel D, Dauner M, Hierlemann H, Hammer C, Kastenbauer E, Planck H. Resorbable polyesters in cartilage engineering: affinity and biocompatibility of polymer fiber structures to chondrocytes. J Biomed Mater Res 1996;33: 57–63.
[8] Nehrer S, Breinan HA, Ramappa A, Shortkroff S, Young G, Minas T, Sledge CB, Yannas IV, Spector M. Canine chondrocytes seeded in type I and type II collagen implants investigated in vitro. J Biomed Mater Res 1997;38:95–104.
[9] Aigner J, Tegeler J, Hutzler P, Campoccia D, Pavesio A, Hammer C, Kastenbauer E, Naumann A. Cartilage tissue engineering with novel nonwoven structured biomaterial based on hyaluronic acid benzyl ester. J Biomed Mater Res 1998;42:172–81.
[10] Madihally SV, Matthew HWT. Porous chitosan scaffolds for tissue engineering. Biomaterials 1999;20:1133–42.
[11] Suh JKF, Matthew HWT. Application of chitosan based polysaccharide biomaterials in cartilage tissue engineering: a review. Biomaterials 2000;21:2589–98.
[12] Gugala Z, Gogolewski S. In vitro growth and activity of primary chondrocytes on a restorable polyactide three-dimensional scaffold. J Biomed Mater Res 2000;49:183–91.
[13] Toolan BC, Frenkel SR, Pachence JM, Yalowitz L, Alexander H. Effects of growth-factor-enhanced culture on a chondrocytes-collagen implant for cartilage repair. J Biomed Mater Res 1996;31:273–80.
[14] Laurencin CT, Norman ME, Elgendy HM, el-Amin SF, Allcock HR, Pucher SR, Ambrosio AA. Use of polyphosphazenes for skeletal tissue regeneration. J Biomed Mater Res 1993;27:963–73.
[15] Saltzman WM, Parsons-Wingerter P, Leong KW, Lin S. Fibroblast and hepatocytes behavior on synthetic polymer surfaces. J Biomed Mater Res 1991;25:741–59.
[16] Hauschka SD, Konigsberg IR. The influence of collagen on the development of muscle colonies. Proc Natl Acad Sci USA 1966;55:119–26.
[17] Bissell MJ, Hall HG, Parry G. How does the extracellular matrix direct gene expression? J Theor Biol 1982;99:31–68.
[18] Ingber D. Extracellular matrix and cell shape: potential control points for inhibition of angiogenesis. J Cell Biochem 1991;47:236–41.
[19] Boudreau N, Myers C, Bissell MJ. From lamini to lamin: regulation of tissue-specific gene expression by the ECM. Trends Cell Biol 1995;5:1–4.
[20] Pierschbacher MD, Ruoslahti E. Cell attachment activity of fibronectin can be duplicated by small synthetic fragments of the molecule. Nature 1984;309:30–3.
[21] Ruoslahti E, Pierschbacher MD. New perspectives in cell adhesion: RGD and integrins. Science 1987;238:491–7.
[22] Massia SP, Hubbell JA. Covalent surface immobilization of Arg-Gly-Asp- and Tyr-Ile-Gly-Ser-Arg-containing peptides to obtain well-defined cell-adhesive substrates. Anal Biochem 1990;187: 292–301.
[23] Lin HB, Sun W, Mosher DF, Garcia-Echeverria C, Schaufelberger K, Lelkes PI, Cooper SL. Synthesis, surface, and cell-adhesion properties of polyurethanes containing covalently grafted RGD-peptides. J Biomed Mater Res 1994;28:329–42.
[24] Graf J, Iwamoto Y, Sasaki M, Martin GR, Kleinman RK, Robey FA, Yamada Y. Identification of an amino acid sequence in laminin mediating cell attachment, chemotaxis, and receprot binding. Cell 1987;48:989–96.
[25] Davis DH, Giannoulis CS, Johnson RW, Desai TA. Immobilization of RGD to ⟨111⟩ silicon surfaces for enhanced cell adhesion and proliferation. Biomaterials 2002;23:4019–27.
[26] Nishiyama Y, Yoshikawa T, Ohara N, Kurita K, Hojo K, Kamada H, Tsutsumi Y, Mayumi T, Kawasaki K. A conjugate from a laminin-related peptide, Tyr-Ile-Gly-Ser-Arg, and chitosan: efficient and regioselective conjugation and significant inhibitory activity against experimental cancer metastasis. J Chem Soc Perkin Trans 1 2000;7:1161–5.
[27] Degim Z, Celebi N, Sayan H, Babul A, Erdogan D, Take G. An investigation on skin wound healing in mice with a taurine-chitosan gel formation. Amino Acids 2002;22:187–98.
[28] Peh K, Khan T, Ching H. Mechanical, bioadhesive strength and biological evaluations of chitosan films for wound dressing. J Pharm Sci 2000;3:303–11.
[29] Nishimura SI. Chemical biology and biomedicine. In: Fraser-Reid BO, Tatsuta K, Thiem J, editors. Glycoscience: chemistry and biology. Berlin: Springer; 2001. p. 1993–2004.
[30] Fu Q, Gowda DC. Carbohydrate-directed conjugation of cobra venom factor to antibody by selective derivatization of the terminal galactose residues. Bioconjugate Chem 2001;12:271–9.
[31] Kratz F, Beyer U, Schumacher P, Krüger M, Zahn H, Roth T, Fiebig HH, Unger C. Synthesis of new maleimide derivatives of daunorubidin and biological activity of acid labile transferrin conjugates. Bioorg Med Chem Lett 1997;7:617–22.
[32] Shinoda M, Kudo T, Suzuki M, Katayose Y, Sakurai N, Saeki H, Kodama H, Fukuhara K, Imai K, Hinoda Y, Matsuno S. Effective adoptive immunotherapy by T-LAK cells retargeted with bacterial superantigen-conjugated antibody to MUC1 in xenografted severe combined immunodeficient mice. Cancer Res 1998;58:2838–43.
[33] Kudryashov V, Kim HM, Ragupathi G, Danishefsky SJ, Livingston PO, Lloyd KO. Immunogenicity of synthetic conjugates of Lewis (y) oligosaccharide with proteins in mice: towards the design of anticancer vaccines. Cancer Immunol Immunother 1998;45:281–6.
[34] Tam JP, Wu CR, Liu W, Zhang JW. Disulfide bond formation in peptides by dimethyl sulfoxide. Scope and applications. J Am Chem Soc 1991;113:6657–62.
[35] Takagi J, Isobe T, Takada Y, Saito Y. Structural interlock between ligand-binding site and stalk-like region of β1 integrin revealed by a monoclonal antibody recognizing conformation-dependent epitope. J Biochem 1997;121:914–21.
[36] Irie A, Kamata T, Puzon-Mclaughlin W, Takada Y. Critical amino acid residues for ligand binding are clustered in a predicted β-turn of the third N-terminal repeat in the integrin α4 and α5 subunits. EMBO J 1995;14:5550–6.
[37] Ishiyama M, Miyazono Y, Sasamoto K, Ohkura Y, Ueno K. A highly water-soluble disulfonated tetrazolium salt as a chromogenic indicator for NADH as well as cell viability. Talanta 1997;44:1299–305.
[38] Kanemura Y, Mori H, Kobayashi S, Islam O, Kodama E, Yamamoto A, Nakanishi Y, Arita N, Yamasaki M, Okano H, Hara M, Miyake J. Evaluation of in vitro proliferative activity of human fetal neural stem/progenitor cells using indirect measurements of viable cells based on cellular metabolic activity. J Neurosci Res 2002;69:869–79.
[39] Nishimura SI, Kohgo O, Kurita K, Kuzuhara H. Chemospecific manipulations of a rigid polysaccharide: synthese of novel chitosan derivatives with excellent solubility in common organic solvents by regioselective chemical modifications. Macromolecules 1991;24:4745–8.
[40] Kurita K, Hashimoto S, Yoshino H, Ishii S, Nishimura SI. Preparation of chitin/polystyrene hybrid materials by efficient graft copolymerization based on mercaptochitin. Macromolecules 1996;29:1939–42.

[41] Iwasaki N, Yamane S, Majima T, Kasahara Y, Minami A, Harada K, Nonaka S, Maekawa N, Tamura H, Tokura S, Shiono M, Monde K, Nishimura SI. Feasibility of polysaccharide hybrid materials for scaffolds in cartilage tissue engineering: evaluation of chondrocyte adhesion to polyion complex fibers prepared from alginate and chitosan. Biomacromolecules 2004;5:828–33.
[42] Albelda SM, Buck CA. Integrins and other cell adhesion molecules. FASEB J 1990;4:2868–80.
[43] Hirsch MS, Lunsford LE, Trinkaus-Randall V, Svoboda KK. Chondrocyte survival and differentiation in situ are integrin mediated. Dev Dyn 1997;210:249–63.
[44] Salter DM, Hughes DE, Simpson R, Gardner DL. Integrin expression by human articular chondrocytes. Br J Rheumatol 1992;31:231–4.
[45] Ostergaard K, Salter DM, Peterson J, Bendtzen K, Hvolris J, Andersen CB. Expression of α and β subunits of the integrin superfamily in articular cartilage from macroscopically normal and osteoarthritic human femoral heads. Ann Rheum Dis 1998;57:303–8.
[46] Dürr J, Goodman S, Potocnik A, von der Mark H, von der Mark K. Localization of β_1-integrins in human cartilage and their role in chondrocyte adhesion to collagen and fibronectin. Exp Cell Res 1993;207:235–44.
[47] Enomoto-Iwamoto M, Iwamoto M, Nakashima K, Mukudai Y, Boettiger D, Pacifici M, Kurisu K, Suzuki F. Involvement of $\alpha_5\beta_1$ integrin in matrix interactions and proliferation of chondrocytes. J Bone Miner Res 1997;12:1124–32.
[48] Wright MO, Nishida K, Bavington C, Godolphin JL, Dunne E, Walmsley S, Jobanputra P, Nuki G, Salter DM. Hyperpolarisation of cultured human chondrocytes following cyclical pressure-induced strain: evidence of a rele for $\alpha_5\beta_1$ integrin as a chondrocyte mechanoreceptor. J Orthop Res 1997;15: 742–7.
[49] Millward-Sadler SJ, Wright MO, Lee HS, Caldwell H, Nuki G, Salter DM. Altered electrophysiological responses to mechanical stimulation and abnormal signaling through $\alpha_5\beta_1$ integrin in chondrocytes from osteoarthritic cartilage. Osteoarthritis Cartilage 2000;8:272–8.
[50] Massia SP, Hubbell JA. Covalently attached GRGD on polymer surfaces promotes biospecific adhesion of mammalian cells. Ann NY Acad Sci 1990;589:261–70.

J Orthop Sci (2005) 10:302–307
DOI 10.1007/s00776-005-0891-y

Original article

Journal of
Orthopaedic Science

Alginate and chitosan polyion complex hybrid fibers for scaffolds in ligament and tendon tissue engineering

Tokifumi Majima[1,2], Tadanao Funakosi[1,2], Norimasa Iwasaki[1,2], Shin-Tarou Yamane[1,2], Kazuo Harada[3], Sachiko Nonaka[3], Akio Minami[1,2], and Shin-Ichiro Nishimura[2,4]

[1]Department of Orthopaedic Surgery, Hokkaido University School of Medicine, Kita 15, Nishi 7, Kita-Ku, Sapporo 060-8638, Japan
[2]Frontier Research Center for Post-genomic Science and Technology, Hokkaido University, Sapporo, Japan
[3]Chemical Biology Institute, Sapporo, Japan
[4]Laboratory of Bio-Macromolecular Chemistry, Division of Biological Sciences, Graduate School of Science, Hokkaido University, Sapporo, Japan

Abstract Selecting the material for a scaffold is critically important for the success of tissue engineering. To simplify complicated biosynthetic matrices and achieve a novel class of potential materials, a model of polyion complex fibers was prepared from alginate and chitosan. In the current in vitro study, we thought that alginate-based chitosan hybrid biomaterials could provide excellent supports for fibroblast adhesion. In the current study, alginate polymer fiber (alginate group) and alginate-based chitosan hybrid polymer fibers (alginate with 0.05% chitosan, alginate-chitosan 0.05% group; alginate with 0.1% chitosan, alginate-chitosan 0.1% group) were originally prepared. We investigated the adhesion behavior of rabbit tendon fibroblast onto alginate polymer fibers versus the adhesion of the fibroblast onto alginate-based chitosan hybrid polymer fibers. Furthermore, mechanical properties and synthesis of the extracellular matrix were investigated. Mechanically, the novel fiber has considerable tensile strength of more than 200 MPa. We demonstrated that the alginate-based chitosan hybrid polymer fibers showed much improved adhesion capacity with fibroblast compared with alginate polymer fiber. Additionally, morphologic studies revealed the dense fiber of the type I collagen produced by the fibroblast in the hybrid polymer fibers. We concluded that an alginate-based chitosan hybrid polymer fiber has considerable potential as a desirable biomaterial scaffold for tendon and ligament tissue engineering.

Introduction

Severe ligament injuries are frequently treated with autograft reconstruction. On the other hand, the use of an autograft results in donor site morbidity. Furthermore, the grafts initially undergo necrosis after implantation. Therefore, the biological grafts often do not provide adequate mechanical strength during the remodeling process.

Offprint requests to: T. Majima
Received: July 26, 2004 / Accepted: January 13, 2005

The tissue engineering approach using biodegradable three-dimensional (3D) scaffolds seeded with cells have more potential alternatives for the treatment of severe ligament and tendon injury.[1] The principal role of the 3D scaffold in tissue engineering is to provide a temporary template with the biomechanical characteristics of the native extracellular matrix (ECM) until the cells produce their own. In addition, the role of scaffolds would be that of a biological stimulator to regulate cell adhesion, growth, migration, differentiation, tissue organization, and matrix remodeling.[2] Cells in a ligament and tendon tissue are embedded in an intricate ECM. Through the cell–ECM adhesions, the ECM transduces physiological signals regulating cell growth, cell proliferation, cell differentiation, and matrix remodeling to the cells. The ECM affects survival, development, shape, polarity, and behavior of cells.[3] The ideal 3D scaffold would mimic the cell environment and manipulate the functional characteristics of a cell to achieve the desired behavior. Thus, selecting the material for such a scaffold is critically important for the success of tissue engineering.

There are some potent biopolymers that can be used as starting materials to prepare stable scaffolds for ligament and tendon tissue engineering.[4–8] Because the biodegradable materials need sufficient mechanical strength until tissue regeneration, collagen, gel,[5] collagen sponge,[7] and collagen construct[4] do not have enough strength for a scaffold in ligament tissue engineering.[2,5] Furthermore, collagen fiber scaffolds suffer from batch-to-batch variability, making consistent reproduction of these constructs difficult.[9] The major limitation is that the collagen scaffold induces an immunogenic reaction.[9] Other scaffolds, such as polyglycolic acid,[7] have limited application because of their mechanical brittleness and the lack of functional groups for signaling molecules.[10]

In the current study, we focused on complicated, 3D networks of ECMs composed of a variety of cell adhe-

sive proteins and proteoglycans. To simplify these complicated biosynthetic matrices and to achieve a novel class of potential materials, a model of polyion complex fibers was prepared from alginate and chitosan. Alginate is one of the naturally abundant and anionic polysaccharides composed of the disaccharide repeating unit [GlcAβ(1–4)Glcβ(1–3)]. Moreover, this polysaccharide is a hyaluronic acid-like biocompatible polymer often used in biomaterials because it contains D-glucuronic acid as a main sugar residue of the repeating unit.[11,12] On the other hand, chitosan has been employed as an excellent biocompatible material for wound healing and tissue repair.[13,14] Because chitosan is regarded as a cationic polysaccharide showing excellent cell adhesive properties,[15] we thought that a hybrid material composed of alginate combined with chitosan might prove to be a novel class of polyion complex effective for scaffolds.

In the present study, we hypothesized that alginate-based chitosan hybrid polymer fibers could provide superior support for fibroblast adhesion compared to that provided by alginate polymer fiber. To test this hypothesis, we investigated the in vitro adhesion behavior of rabbit tendon fibroblast onto alginate-based chitosan hybrid polymer fibers. The objectives of this in vitro study were to determine the material properties of the alginate-based chitosan hybrid polymer fiber and to evaluate fibroblast adhesion and ECM synthesis in the novel polymer fiber.

Materials and methods

Preparation of polyion complex fiber

A solution of sodium alginate (4% w/w; mol. wt 600000; D-mannuronic acid/L-guluronic acid ratio 1.0) (Kibun Food Chemifa, Tokyo, Japan) and chitosan oligomer (0, 0.5, or 0.1% w/w, mol. wt. 18000, degree of deacetylation of ~70%) (Kimitsu Chemical, Tokyo, Japan) in water was used. The process of preparing the fibers using the original apparatus was reported previously.[16] Briefly, dope of alginate was spun into a coagulation system (first coagulation bath: 0.05% chitosan or 0.1% chitosan; second coagulation bath: 3% $CaCl_2$ in water-MeOH) through a nozzle containing 50 holes, each with a diameter of 0.1 mm. The fibers were washed with methanol and dried at room temperature; they were then used for further experiments after sterilization. In the current study, alginate polymer fiber (alginate group) and alginate-based chitosan hybrid polymer fibers (alginate with 0.05% chitosan, alginate-chitosan 0.05% group; alginate with 0.1% chitosan, alginate-chitosan 0.1% group) were originally prepared.

In a preliminary experiment, we found that the concentration of chitosan on the alginate fiber depended on the concentration of chitosan coagulation bath up to 0.1%. However, the concentration on the alginate fiber did not increase when the concentration of the chitosan coagulation bath increased to more than 0.1%. Furthermore, chitosan is a cationic polysaccharide consisting of glucosamine residues. The calcium ion and chitosan exist in the first coagulation bath. The strength of alginate fibers would decrease owing to the inhibition of chelation of calcium ion with alginate chains at higher concentrations of chitosan. Therefore, in this study, we did not prepare the hybrid fibers coated with more than 0.1% chitosan concentration.

Polymer fiber of Polyglactin 910 — a 90:10 copolymer of glycolide and lactide, coated with polyglactin 370 and calcium stearate (9-0 Vicryl suture material (Ethicon, Somerville, NJ, USA) USA) — was also used as a control material. This fibrous material, which has the same diameter as the novel fibers, has been widely used in clinical fields.

Measurement of material properties

Material properties of each fiber were measured according to the Japanese Industrial Standards (JIS) L1015 in a dry condition (room temperature 22° ± 2°C, humidity 50%). Tensile tests for five samples of each material were performed at a crosshead speed of 20 mm/min using the material testing machine (P/N346-51299-02; Shimadzu, Kyoto, Japan). The cross-sectional area was determined using a microscope (BX50; Olympus, Tokyo, Japan) and a video dimension analyzer (VM-30; Olympus). After material testing, the water content of the polymer fiber was 15.76% in the alginate group, 16.56% in the alginate-chitosan 0.05% group, and 16.42% in the alginate-chitosan 0.1% group.

Cell preparation

Fibroblasts were isolated from the patellar tendon of a Japanese white rabbit under sterile conditions as described by Nagineni et al.[17] The culture medium used in the present study was made from Dulbecco's modified Eagle's medium (D5796; Sigma, St. Louis, MO, USA), 10% fetal bovine serum (10099-141; Invitrogen, Carlsbad, CA, USA), 100× concentrated of Penicillin-Streptomycin-Fungizone mixture (17-745H; Biowhittaker Walkersville, MD, USA) (medium I). Cells were incubated at 37°C in a humidified atmosphere of 5% CO_2 and supplemented at 3-day intervals with medium I. Three weeks after preparing the culture, the explanted pieces of the patellar tendon were discarded and the outgrown cells were removed with trypsin-EDTA for subculture. Cells were maintained in the culture using standard procedures at a second passage. The fibroblasts suspension was concentrated to 1.4 ×

Table 1. Material properties of each fiber

Material	Tensile strength (MPa)	Strain at failure (%)
Control	886.2 ± 7.7	28.1 ± 0.6
Alginate	274.1 ± 4.9*	9.0 ± 0.4*
Alginate/chitosan 0.05%	221.7 ± 5.4*	10.6 ± 0.7*
Alginate/chitosan 0.1%	235.2 ± 8.5*	12.3 ± 0.3*

* $P < 0.05$ vs. control ($n = 5$, mean ± SD)

10^7 cells/ml using a hemocytometer, and the viability of the fibroblasts was found to be more than 95%, as determined by the trypan blue indicator method.

Cell adhesion study

The cell adhesion study was performed according to a previous repore.[18] Briefly, the fibrous samples were cut into 7 mm lengths and packed in a Teflon tube (30 mm length, 7 mm inner diameter). Then 0.1 ml of the fibroblast suspension (1.4×10^7 cells/ml) was loaded onto the column. The cells were allowed to adhere in a humidified incubator for 1 h. Each column was rinsed with 1 ml of phosphate-buffered saline, and the unattached cells were quantified by the microscopic observation of the rinse solution. Five samples for each of the polymer fibers were measured.

Histological observation

Cell proliferation and ECM production were observed by light microscopy 14 days after the culture in three types of 3D scaffolds. Moreover, scanning electron microscopy (SEM) observations were performed 14 days after culture. Specimens were also evaluated immunohistochemically for type I and type III collagen production 14 days after culture.

For SEM (S-4500; Hitachi, Tokyo, Japan) observation, samples were rinsed with Ringer's solution to remove unattached cells at the end of the incubation period. The cells on the scaffold were fixed overnight with 2.5% glutaraldehyde supplemented with 0.1 M phosphate buffer. After fixation, the SEM specimens were rinsed with phosphate buffer and fixed in 1% OsO_4 for 1 h and then soaked in 1% tannic acid for an additional 1 h. These procedures were repeated three times. The specimen was dehydrated, mounted on an aluminum stub, and then coated with argon using an ion coater (HCP-2; Hitachi, Tokyo, Japan) for observation.

For immunohistochemical observation, the samples were stored in deep-frozen conditions. Frozen sections of 8 μm were cut, mounted on microscope slides, thawed, and fixed with acetone for 5 min at −20°C. After drying, the sections were hydrated with a solution of phosphate-buffered saline for 5 min. The cells and scaffolds were incubated with the primary antibodies, a mouse monoclonal antibody to human collagen type I (1:100), type II (I:100), and type III (1:100) (Fuji Chemicals, Takaoka, Japan), for 60 min at room temperature. The sections were washed three times and incubated with the peroxidase-labeled polymer-conjugated anti-rabbit antibody (Envision System; Dako, Carpinteria, CA, USA) for 1 h. The reaction was developed with a 3,3′-diaminobenzidine tetrahydrochloride (DAB) (Sigma) solution.

Statistical analysis

Statistical comparisons were performed for the material properties and cell adhesion study using one-way analysis of variance (ANOVA) and Fisher's protected least significant differences (PLSD) test. The significance level was set at 0.05.

Results

Material properties

The material properties of each fiber are shown in Table 1. The tensile strength of each fiber group was 274.1 MPa in the alginate group, 221.7 MPa in the alginate-chitosan 0.05% group, and 235.2 MPa in the alginate-chitosan 0.1% group. The mean tensile strengths of all the new materials were significantly lower than that of a control polyglactin fiber ($P < 0.05$). The strain at failure was 9.0% in the alginate group, 10.6% in the alginate-chitosan 0.05% group, and 12.3% in the alginate-chitosan 0.1% group. Strain at failure in the control fiber was significantly higher than that of the new polymer fibers ($P < 0.05$) (Table 1). There were no significant differences in the tensile strength or strain at failure between the alginate group and alginate-chitosan groups.

Cell adhesion

As shown in Fig. 1, the numbers of unattached cells in the alginate-chitosan groups were significantly lower than that in the control ($P < 0.001$) and alginate ($P < 0.05$) groups. There was no significant difference

between the alginate-chitosan 0.05% group and the alginate-chitosan 0.1% group.

Cell morphology

The SEM observations showed that the fibroblasts spread on the polymer fibers directly produced collagen fibril-like matrices on the polymer fiber. The length of the cell was 20–50 μm (Fig. 2). There was no effect of the composition of the polymer fiber on cell morphology after 14 days in culture.

Immunostaining for type I collagen was prominent around the alginate-chitosan 0.1% polymer fibers 14 days after the culture (Fig. 3A). Type I collagen was more abundant around the surface of the polymer fiber. Type II collagen was not stained around the surface of the scaffold. Immunolabeling for type III collagen was not clear around the polymer fibers 14 days after culture (Fig. 3B). There were no significant differences in staining among the three types of scaffold.

Discussion

The study demonstrated that the adhesivity of fibroblasts is significantly higher on the alginate-based chitosan hybrid polymer fiber than on the alginate polymer fiber. Madihally and Matthew[19] reported that the cationic nature of chitosan allowed electrostatic interactions with anionic GAGs, proteoglycans, and other

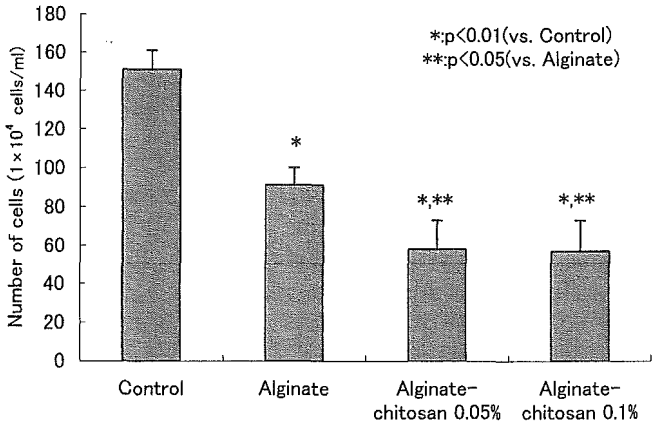

Fig. 1. Number of washed-out fibroblasts from control, alginate, and alginate-based chitosan hybrid polymer fibers. Chitosan coating significantly reduced the number of unattached cells ($P < 0.05$)

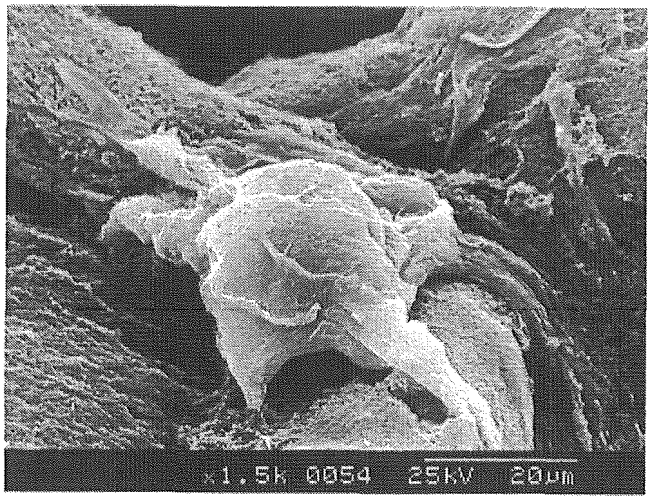

Fig. 2. Scanning electron micrograph of rabbit fibroblast seeded on alginate-based 0.1% chitosan hybrid fiber after 14 days of culture

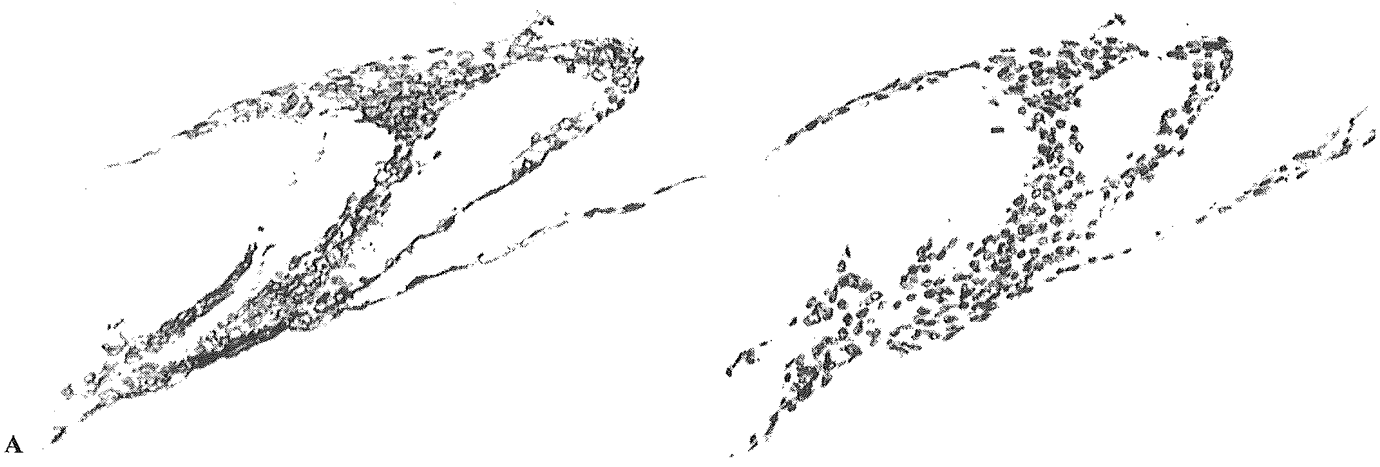

Fig. 3. Photographs of immunostaining for type I and type III collagen in the alginate-based 0.1% chitosan hybrid polymer fibers 14 days after culture. Type I collagen was more abundant, and type II collagen was not detected around the fibers. **A** Type I collagen staining. **B** Type III collagen staining. **A,B** ×200

negatively charged species. These ionic interactions may serve as a mechanism for retaining and recruiting cells, growth factors, and cytokines in a tissue scaffold. Consequently, alginate-based chitosan hybrid polymer has great potential as a desirable biomaterial for tissue scaffolds.[20–22]

There was no significant difference in material proerties between alginate and alginate/chitosan hybrid fibers. It has been reported that congelation of sodium alginate solution occurred with egg box formation, which is produced by chelate combination between carboxyl residue of alginate and calcium ions.[23] In the first coagulation bath, the concentration of calcium ion is much higher than that of chitosan. The difference in concentration of chitosan and calcium ion leads to a dominant reaction between alginate and calcium ions. This may be the reason why coating of chitosan did not change the material properties of alginate.

A scaffold for ligament and tendon tissue engineering requires adequate mechanical strength to maintain the initial shape of the implanted scaffold. During the development of the novel fiber, one of the most critical points was to increase the mechanical strength of the fiber for 3D fabrication. The obtained material properties of the novel fibers indicate enough mechanical strength to create a 3D fabricated scaffold. The hybrid polymer fibers in our study can be fabricated to obtain the desirable mechanical strength and shape. For example, the failure load of 8 mm diameter fabricated hybrid fibers is approximately 10000 N. This is about five times greater than the failure load of the anterior cruciate ligament; the ultimate load of young anterior cruciate ligament is 2160 N.[24] This novel fabric consisting of alginate-chitosan hybrid polymer fiber may serve as an ideal scaffold with adequate strength for ligament and tendon tissue engineering.

The novel fibers provided a suitable support for ECM production. In a normal ligament, more than 90% of collagen consists of type I collagen, with a low percentage of type III collagen.[25,26] On the other hand, injured ligament and tendon contains more type III collagen, which is mechanically weak.[25,26] In the present study, seeded fibroblasts in an alginate and chitosan hybrid polymer fiber scaffold produced type I collagen predominantly. These results indicated that the novel hybrid fibers might offer a superior environment for ligament and tendon tissue engineering. The quantitative studies concerning ECM products in the 3D culture should be further examined.

One of the limitations of the present study is that the mechanical strength of the fibers in vivo has remained unknown. Tamura et al. reported that chitosan-coated alginate filament significantly depends on the chitosan molecular weight, especially in wet properties, because of tight ionic interaction of chitosan with alginate filament.[27] They also reported that tensile strength in the wet condition decreased around 40% of that in dry condition. Mechanical strength of alginate fiber is maintained by crosslinking of calcium ion. When the alginate fiber is implanted in vivo, calcium ion is replaced by natrium ion, following which the alginate fiber degrades. On the other hand, chitosan coating suppresses this degradation because the replacement of calcium ion in alginate fiber is interrupted. Our strategy for soft tissue regeneration is not to reconstruct it with a synthetic nonbioabsorbable graft but to replace it with tissue ingrowth using a bioabsorbable scaffold seeded with cells. In line with this strategy, in vivo biocompatibility and biodegradability of the hybrid fibers should be studied. Although the biodegradability of these hybrid polymer fibers remains unclear, we can adjust the degradation rate of the fibers by manipulating the degree of deacetylation in chitosan fibers or fabrication of hybrid fiber.

Conclusions

Introducing chitosan into the fundamental scaffold material for tissue engineering increased cell adhesive potential and biological effects on the cultured fibroblast. Therefore, the alginate-based chitosan hybrid polymer fibers have potential as a scaffold material for ligament tissue engineering.

Acknowledgments. This work was supported by a Grant-in-Aid for Scientific Research from the Japan Ministry of Education, Culture, Sports, Science, & Technology (B-1539044) and a Grant-in-Aid for New Energy and Industrial Technology Development Organization (03A04002a).

References

1. Langer R, Vacanti JP. Tissue engineering. Science 1993;260:920–7.
2. Hynes RO. Cell adhesion: old and new questions. Trends Cell Biol 1999;9:M33–7.
3. Iozzo RV, Murdoch AD. Proteoglycans of the extracellular environment: clues from the gene and protein side offer novel perspectives in molecular diversity and function. FASEB J 1996;10:598–614.
4. Dunn MG, Liesch JB, Tiku ML, Zawadsky P. Development of fibroblast-seeded ligament analogs for ACL reconstruction. J Biomed Mater Res 1995;29:1363–71.
5. Gentleman E, Lay AN, Dickerson DA, Nauman EA, Livesay GA, Dee KC. Mechanical characterization of collagen fibers and scaffolds for tissue engineering. Biomaterials 2003;24:3805–13.
6. Huang D, Chang TR, Aggarwal A, Lee RC, Ehrlich P. Mechanisms and dynamics of mechanical strengthening in ligament-equivalent fibroblast-populated collagen matrices. Ann Biomed Eng 1993;21:289–305.
7. Ibarra C, Cao Y, Vacanti JP, Kim TH, Vacanti CA. Tissue engineering ligaments. Surg Forum 1996;47:612–5.

8. Quteish D, Singh G, Dolby AE. Development and testing of a human collagen graft material. J Biomed Mater Res 1990;24:749–60.
9. Koski JA, Ibarra C, Rodeo SA. Tissue-engineered ligament. Orthop Clin North Am 2000;31:437–52.
10. Zhu H, Ji J, Lin R, Gao C, Feng L, Shen J. Surface engineering of poly (D,L-lactic acid) by entrapment of chitosan-based derivatives for the promotion of chondrogenesis. J Biomed Mater Res 2002; 62:532–9.
11. Dar A, Shachar M, Leor J, Cohen S. Optimization of cardiac cell seeding and distribution in 3D porous alginate scaffolds. Biotechnol Bioeng 2002;80:305–12.
12. Jianqi H, Hong H, Lieping S, Genghusf G. Comparison of calcium alginate film with collagen membrane for guided bone regeneration in mandiburlar defects in rabbits. J Oral Maxillofac Surg 2002;60:1449–54.
13. Degim Z, Celebi N, Sayan H, Babul A, Erdogan D, Take G. An investigation on skin wound healing in mice with a taurine-chitosan gel formulation. Amino Acids 2002;22:187–98.
14. Khan TA, Peh KK, Ching HS. Mechanical, bioadhesive strength and biological evaluations of chitosan films for wound dressing. J Pharm Pharmacent Sci 2000;3:303–11.
15. Howling GI, Dettmar PW, Goddard PA, Hampson FC, Dornish M, Wood EJ. The effect of chitin and chitosan on the proliferation of human skin fibroblasts and keratinocytes in vitro. Biomaterials 2001;22:2959–66.
16. Yamane S, Iwasaki N, Majima T, Funakosi T, Masuko T, Harada K, et al. Feasibility of chitosan-based hyaluronic acid hybrid biomaterial for a novel scaffold in cartilage tissue engineering. Biomaterials 2005;26:611–9.
17. Nagineni CN, Amiel D, Green MH, Berchuck M, Akeson WH. Characterization of the intrinsic properties of the anterior cruciate and medial collateral ligament cells: an in vitro cell culture study. J Orthop Res 1992;10:465–75.
18. Nishimura S, Nishi N, Tokura S. Adhesion behaviour of murine lymphocytes on the surface of fibrous chitin and its derivatives. Int J Biol Macromol 1985;7:100–4.
19. Madihally SV, Matthew HWT. Porous chitosan scaffolds for tissue engineering. Biomaterials 1999;20:1133–42.
20. Chung TW, Yang J, Akaike T, Cho KY, Nah JW, Kim SI, et al. Preparation of alginate/galactosylated chitosan scaffold for hepatocyte attachment. Biomaterials 2002;23:2827–34.
21. Sakai S, Ono T, Ijima H, Kawakami K. Control of molecular weight cut-off for immunoisolation by multilayering glycol chitosan-alginate polyion complex on alginate-based microcapsules. J Microencapsul 2000;17:691–9.
22. Wang L, Khor E, Lim LY. Chitosan-alginate-$CaCl_2$ system for membrane coat application. J Pharm Sci 2001;90:1134–42.
23. Grant GT, Morris ER, Rees DA, Smith PJC, Thom D. Biological interactions between polysaccharides and divalent cations: the egg-box model. FEBS Lett 1973;32:195–8.
24. Woo S L-Y, Hollis JM, Adams DJ, Lyon RG, Takai S. Tensile properties of the human femur-anterior cruciate ligament-tibia complex. The effects of specimen age and orientation. Am J Sports Med 1991;19:217–25.
25. Frank C, Amiel D, Woo SL-Y, Akeson W. Normal ligament properties and ligament healing. Clin Othhop 1985;196: 15–25.
26. Lo IKY, Randle JA, Majima T, Thornton G, Rattner JB, Shrive NG, et al. New directions in understanding and optimizing ligament and tendon healing. Curr Opin Orthop 2000;11:421–8.
27. Tamura H, Tsuruta Y, Tokura S. Preparation of chitosan-coated alginate filament. Mater Sci Eng 2002;C20:143–7.

Application of Tissue Engineering Techniques for Rotator Cuff Regeneration Using a Chitosan-Based Hyaluronan Hybrid Fiber Scaffold

Tadanao Funakoshi,*[†‡] MD, PhD, Tokifumi Majima,[†‡] MD, PhD, Norimasa Iwasaki,[†‡] MD, PhD, Naoki Suenaga,[†] MD, PhD, Naohiro Sawaguchi,[†‡] MD, Kazumi Shimode,[†‡] MD, Akio Minami,[†‡] MD, PhD, Kazuo Harada,[§] PhD, and Shin-ichiro Nishimura,[‡‖] PhD

From the [†]Department of Orthopaedic Surgery, Hokkaido University, Graduate School of Medicine, Sapporo, Japan, [‡]Frontier Research Center for Post-genomic Science and Technology, Hokkaido University, Sapporo, Japan, [§]Chemical Biology Institute Inc, Sapporo, Japan, and [‖]Laboratory of Bio-macromolecular Chemistry, Hokkaido University, Graduate School of Science, Sapporo, Japan

Background: The current surgical procedures for irreparable rotator cuff tears have considerable limitations. Tissue engineering techniques using novel scaffold materials offer potential alternatives for managing these conditions.

Hypothesis: A chitosan-based hyaluronan hybrid scaffold could enhance type I collagen products with seeded fibroblasts and thereby increase the mechanical strength of regenerated tendon in vivo.

Study Design: Controlled laboratory study.

Methods: The scaffolds were created from chitosan-based hyaluronan hybrid polymer fibers. Forty-eight rabbit infraspinatus tendons and their humeral insertions were removed to create defects. Each defect was covered with a fibroblast-seeded scaffold (n = 16) or a non-fibroblast-seeded scaffold (n = 16). In the other 16 shoulders, the rotator cuff defect was left free as the control. At 4 and 12 weeks after surgery, the engineered tendons were assessed by histological, immunohistochemical (n = 2), and biomechanical (n = 6) analyses.

Results: Type I collagen was only seen in the fibroblast-seeded scaffold and increased in the regenerated tissue. The tensile strength and tangent modulus in the fibroblast-seeded scaffold were significantly improved from 4 to 12 weeks postoperatively. The fibroblast-seeded scaffold had a significantly greater tangent modulus than did the non-fibroblast-seeded scaffold and the control at 12 weeks.

Conclusion: This scaffold material enhanced the production of type I collagen and led to improved mechanical strength in the regenerated tissues of the rotator cuff in vivo.

Clinical Relevance: Rotator cuff regeneration is feasible using this tissue engineering technique.

Keywords: chitosan; hyaluronan (HA); tissue engineering; rotator cuff; scaffold

The rotator cuff has limited healing potential for massive tears. Therefore, various surgical techniques, including musculotendinous transfers and patch grafts using biological or synthetic materials, have been used for the treatment of irreparable tears.[18,25] However, musculotendinous transfers result in donor site morbidity, and patch grafts become mechanically weaker over time as they cause adverse reactions. New strategies to treat irreparable rotator cuff tears must therefore be developed.

Tissue engineering is an emerging scientific approach that attempts to develop biological substitutes constructed from isolated cells and 3-dimensional (3D) polymeric scaffolds.[17] Some naturally occurring materials, including collagen gels, collagen sponges, collagen constructs, and silks,

*Address correspondence to Tadanao Funakoshi, MD, PhD, Department of Orthopaedic Surgery, Hokkaido University School of Medicine, Kita 15 Nishi 7 Kita-ku, Sapporo 060-8638, Japan (e-mail: t-funa@med.hokudai.ac.jp).

Presented in part at the 50th annual meeting of the Orthopaedic Research Society, San Francisco, California, March 2004.

No potential conflict of interest declared.

The American Journal of Sports Medicine, Vol. 33, No. 8
DOI: 10.1177/0363546504272689

have been developed to construct scaffolds of ligaments and tendons.[1,4,8,9,12,30] Awad et al[4] reported that the repair of patellar tendon injuries treated with mesenchymal stem cells and collagen gel composition achieved twice the structural properties of the contralateral gap controls. Altman et al[1] reported the success of ligament tissue regeneration using bone marrow stem cell–seeded silk materials. Although these studies have shown the feasibility of tissue engineering techniques for the regeneration of ligaments or tendons, there are still a number of limitations to the clinical application of these engineering techniques.

One of the most important considerations is that implanted tissue, including a biodegradable scaffold material, must increase the mechanical strength by augmenting the extracellular matrices (ECMs) produced by seeded cells during the process of tissue regeneration. A strategy for achieving this ideal process is to develop a scaffold material that can enhance this process and mechanically support the regeneration process. To our knowledge, there is no presently available ideal scaffold material for the tissue engineering of ligaments and tendons.

The main component of ECMs in ligaments and tendons is type I collagen. The mechanical properties of regenerated tissues, which predominantly consist of type III collagen, are likely to be inferior to those of the native tissues.[2,10] Therefore, to improve the mechanical properties of regenerated tendon, it is essential to increase type I collagen content in the regenerated tissues.

We have recently developed a novel chitosan-based hyaluronan (HA) hybrid polymer fiber.[29] An in vitro trial demonstrated that this novel material provided excellent support for cultured fibroblast adhesion and type I collagen production.[11] In addition, the mechanical strength of this fiber can make it possible to create a 3D fabricated scaffold. We have developed a novel 3D scaffold based on this material for rotator cuff regeneration. The hypotheses of this study are that this novel scaffold could enhance type I collagen production with seeded fibroblasts and increase the mechanical strength of the regenerated tendons in vivo. To test these hypotheses, we created rabbit models of rotator cuff defects and treated them with tissue engineering techniques using this scaffold material. We aimed to measure the production of type I collagen as a main component of the regenerated rotator cuff and to evaluate any alterations in the mechanical properties of the regenerated tissues. The results obtained here should thus provide fundamental information on the in vivo interactions between fibroblasts and this novel scaffold material for rotator cuff regeneration.

MATERIALS AND METHODS

Preparation of 3D Chitosan-Based HA Hybrid Polymer Fiber Scaffold

Chitosan-based HA hybrid polymer fibers were developed by the wet spinning method that has been previously described.[11,29] The chitosan dope was spun into a calcium coagulant through a stainless steel spinneret. A 50% aqueous methanol solution was used for a second coagulation bath, and 0.1% HA dissolved in 50% aqueous methanol solution was used for a third coagulation bath. All 3 coagulation baths were performed at room temperature. The concentration of HA used was based on its potential for adhering to the fibers and on its mechanical properties according to an in vitro trial study.[11] The fiber wound in the roller was washed in 90% aqueous methanol and dried at room temperature. We twisted 2 threads of the chitosan-based HA fibers together to make a string using a twister machine (AMT-2; Marui Textile Machinery Co, Osaka, Japan). Two such strings were further twisted in the opposite direction to make 1 braid. The scaffold (10 mm in length, 7 mm in width, and 0.7 mm in thickness) was created from 13 braids using a braiding machine in the ratio of 80:30 (rotation to sending; 102-C; Kokubun Limited Co, Shizuoka, Japan) (Figure 1A). The angle between each braided fiber was 100° (Figure 1B). The 3D materials were sterilized in an autoclave at 135°C for 20 minutes before adding fibroblast cultures. The mechanical properties of the 3D scaffold were measured according to Japanese Industrial Standards L1015 under dry conditions. In addition, to test the degradability of the scaffold, the properties were evaluated again after 4 weeks of incubation in the standard medium, as mentioned below.

Fibroblast Culture in 3D Scaffold

Fibroblasts were isolated from the patellar tendon of a Japanese White rabbit under sterile conditions as described by Nagineni et al.[22] The patellar tendon is easier to manipulate than is the rotator cuff tendon. The peritendinous tissues were carefully removed to avoid cellular contamination. The culture medium used in the present study was Dulbecco's modified Eagle's medium (D5796; Sigma Chemical Co, St Louis, Mo), with 10% fetal bovine serum (10099-141; Invitrogen Corp, Carlsbad, Calif) and 100 IU/mL penicillin, 100 μg/mL streptomycin, and 0.25 μg/mL fungizone (17-745H; Biowhittaker, Walkersville, Md). Cells were incubated at 37°C in a humidified atmosphere of 5% CO_2 and supplemented at 3-day intervals with fresh culture medium. Three weeks after culturing, the explanted pieces of patellar tendon were discarded, and the outgrown cells were removed for subculture using trypsin digestion. The fibroblasts were used at a second passage in this study. Cell viability was more than 95%, as determined by trypan blue exclusion. A 50-mL aliquot of the fibroblast suspension (8.0×10^6 cells/mL) was loaded onto each 3D scaffold. The materials were used for the cell-seeded scaffold (CSS) after 4 weeks of culture.

Study Design and Surgical Procedure

Animal experimentations were approved by institutional animal care committees. Forty-eight shoulders in 24 mature female Japanese White rabbits weighing 3.2 ± 0.2

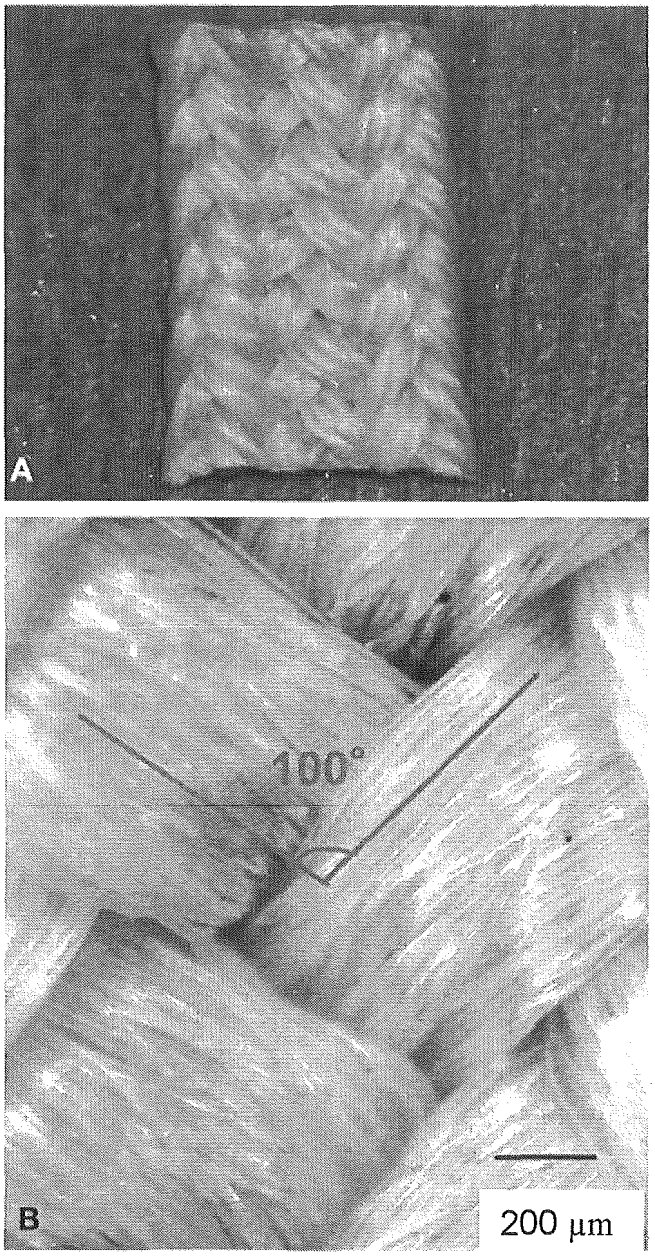

Figure 1. A, 3-dimensional scaffold (10 mm in length, 7 mm in width, and 0.7 mm in thickness) was created from 13 braids using a braiding machine. B, the angle between each braided fiber was 100°.

kg (mean ± SE) were used. Under general anesthesia using intravenous pentobarbital (0.05 mg/kg) followed by isoflurane in oxygen gas anesthesia, the infraspinatus tendon and its humeral insertion were removed to create a defect of 10 × 7 mm in length and width. A trough was created in the cortical bone over the insertion of the infraspinatus tendon until cancellous bone was exposed. In 16 right shoulders, the defects were covered with 10 × 7-mm patches of the CSS (CSS group) (Figure 2). The distal ends of the scaffolds were fixed into the bony trough with two 3-0 nylon mattress sutures. The proximal stumps of the scaffolds were then sutured to the infraspinatus tendons using the same technique. The 4 sides of the scaffolds were further sutured to define the area of implantation. In the 16 contralateral shoulders, the defects were covered with the non-cell-seeded scaffold (NCSS group) using a similar procedure. In the other 16 shoulders in 8 rabbits, the rotator cuff defects were left free as controls (control group). After surgery, the animals were not immobilized and were allowed to move freely in their cages.

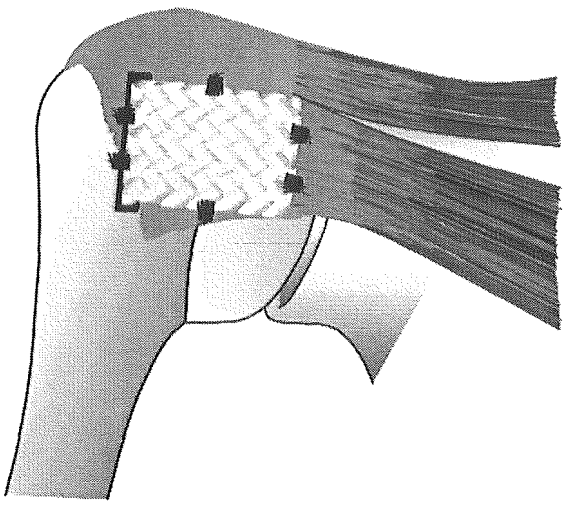

Figure 2. Surgical procedure. The infraspinatus tendons from a rabbit were removed to create the defects. A bony trough was created over the insertion of the infraspinatus tendon, and a scaffold was inserted.

Histological and Immunohistochemical Observation

Two rabbits were sacrificed using intravenous pentobarbital overdoses at each time period (4 and 12 weeks) for histological and immunohistochemical analyses. En bloc specimens, including the greater tuberosity, were harvested from each shoulder. The specimens were fixed in 10% buffered formalin and decalcified in formaldehyde and formic acid. They were longitudinally split to obtain full-thickness sections from the regenerated tissues. The sections were embedded in paraffin wax, cut into 5-mm-thick longitudinal sections, and stained with hematoxylin and eosin. For immunohistochemistry, we used mouse monoclonal antibodies for human type I, type II, and type III collagen (1:100; Fuji-Chemicals, Takaoka, Japan).[16] The sections were washed 3 times and incubated with peroxidase-labeled, polymer-conjugated antirabbit antibody (Envision System; DakoCytomation California Inc, Carpinteria, Calif) for 60 minutes. The peroxidase reaction was developed using 3,3'-diaminobenzidine tetrahydrochloride.

Measurement of Mechanical Properties

At 4 and 12 weeks after surgery, 6 shoulders in each group were obtained for biomechanical evaluation. The speci-

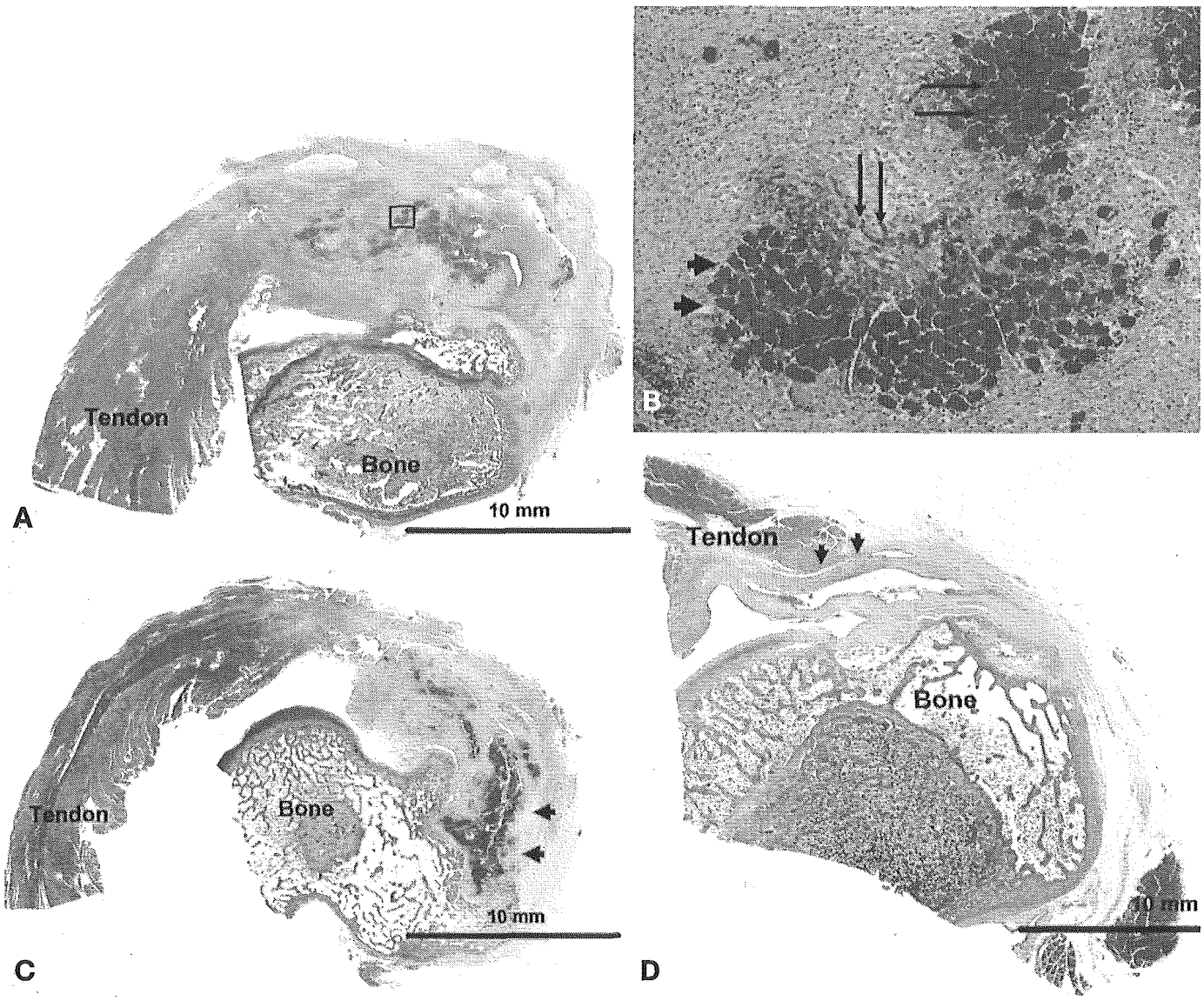

Figure 3. Micrographs of each group 4 weeks after surgery. A, cell-seeded scaffold (hematoxylin and eosin staining). B, cell-seeded scaffold (hematoxylin and eosin staining, original magnification ×100). Hybrid fibers have not been absorbed (short black arrows). Although many fibroblasts and macrophages were observed, there was no severe immune reaction (long black arrows). Collagen fibers were not observed. C, non-cell-seeded scaffold (hematoxylin and eosin staining). Note that there were no significant differences in cell numbers and collagen formation in the scaffolds with or without cells (black arrows). D, control defect (hematoxylin and eosin staining). Note that only a thin membrane was present (black arrows).

mens were wrapped in gauze wetted with physiological saline solution, covered with plastic film, and stored at −32°C until the start of biomechanical testing. Before tensile testing, each shoulder was thawed overnight at 4°C. The rotator cuff–humerus complex was dissected, and its surrounding tissues were carefully removed, referring to the 4-corner suture makers. The cross-sectional area of each regenerated tendon was measured by the contact method using an area micrometer (2050F-60; Mitutoyo, Tokyo, Japan), as described previously.[20] A bone-tendon preparation was mounted and attached to a conventional tensile tester (P/N346-51299-02; Shimadzu, Kyoto, Japan). The regenerated tendon site in each specimen was cut to create a dumbbell shape 3 mm wide for biomechanical study. The free end of the tendon was secured with a specially designed cryo-jaw device.[26] The mechanical testing protocol was based on a previous report.[20] After a preload of 0.5 N was applied for 10 minutes, the specimen was subjected to 10 cycles of loading and unloading for preconditioning with between 0 and 0.5 mm of crosshead displacement. Tensile tests in all specimens were performed at a crosshead speed of 20 mm/min. A stress-strain curve was obtained from the load-displacement relationship, in which stress was calculated by dividing the tensile load by initial cross-sectional area, and strain was calculated by dividing the displacement by initial gauge length. Tensile

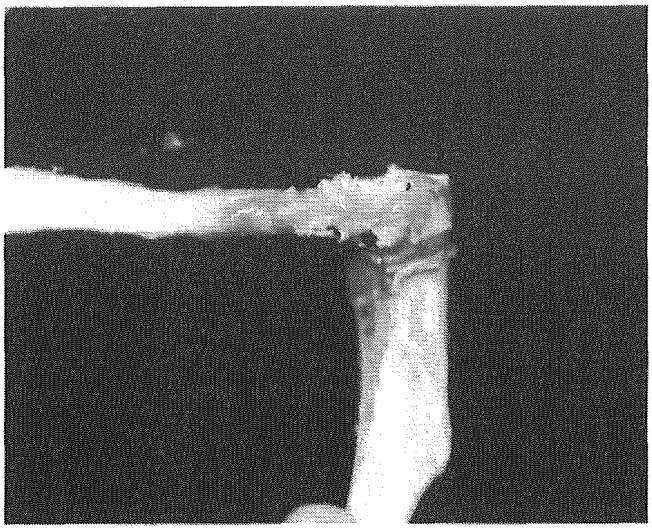

Figure 4. The gross appearance of the cell-seeded scaffold 12 weeks after surgery. Note the good continuity with the infraspinatus muscles and their insertions.

strengths and tangent moduli were determined from stress-strain relationships. The tangent modulus was defined by the slope of the stress-strain curve, which was determined by a least squares linear regression analysis of the data between the end point of the toe region and that point starting to bend before failure.

Statistical Analysis

Statistical comparisons were performed using 1-way analysis of variance and the Fisher protected least significance post hoc test; $P < .05$ was assumed as significant. All data are presented as mean ± SE.

RESULTS

Mechanical Properties of 3D Scaffold

The ultimate strength and stiffness of the scaffold under dry conditions were 67.2 ± 2.2 N and 18.8 ± 1.2 N/mm, respectively. At 4 weeks after incubation, the same measures were 16.0 ± 1.6 N and 6.8 ± 0.8 N/mm, respectively. The cross-sectional area of the scaffold was 0.936 mm^2 (1 thread; 18 000 μm^2, 52 threads). Therefore, the tensile strength of the scaffold was theoretically 72.0 MPa under dry conditions and 17.0 MPa at 4 weeks after incubation, based on the ratio of the ultimate strength to the cross-sectional area (0.936 mm^2).

Histological and Immunohistochemical Evaluation

4-Week Specimens. Macroscopically, in both the CSS and NCSS groups, the defects were covered with thin scar-like tissues on the implanted scaffold. However, there was no tissue covering the defect in the control group. Microscopically, at this point, there were no significant dif-

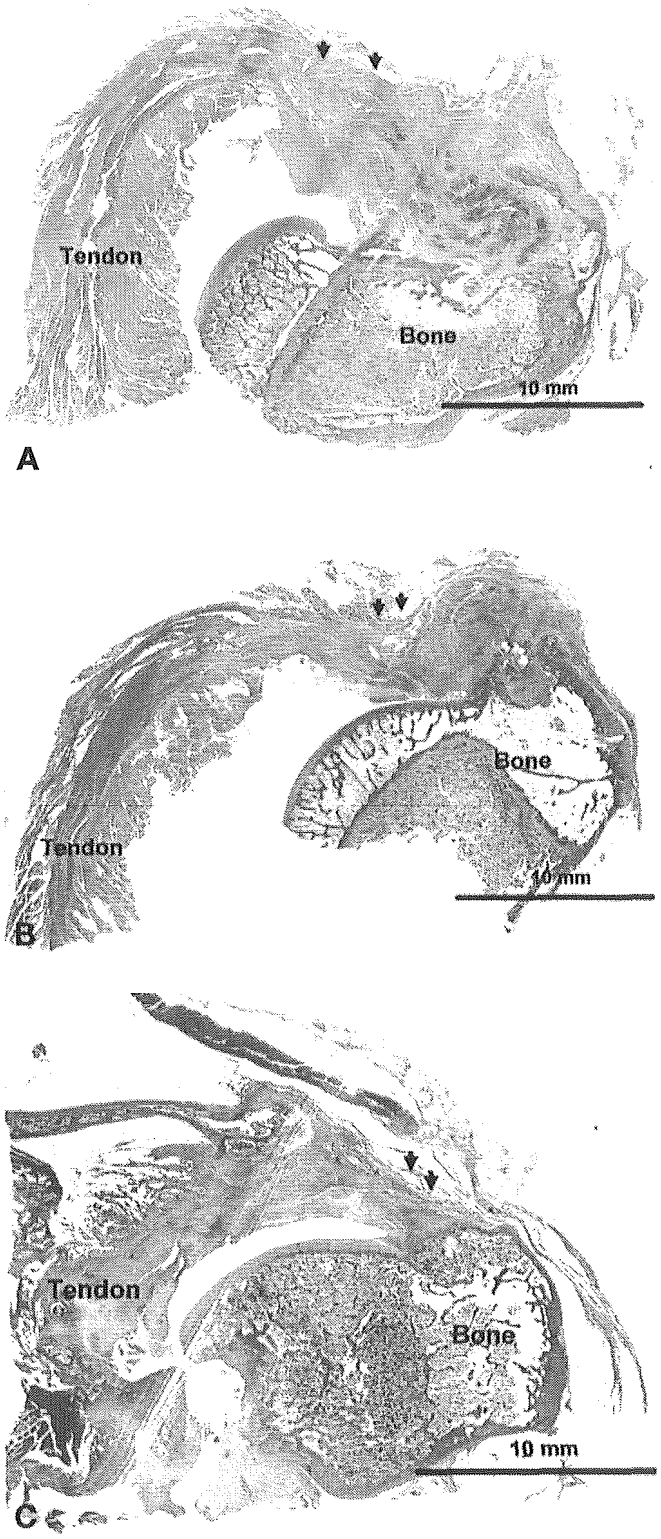

Figure 5. Micrographs of each group 12 weeks after surgery (hematoxylin and eosin staining). A, cell-seeded scaffold. Note the well-aligned collagen fibers (black arrows). B, non-cell-seeded scaffold. Note the unaligned collagen fibers (black arrows). C, control. Note that thin membranes with many fibroblasts linked the end of the torn cuff and the bone (black arrows).

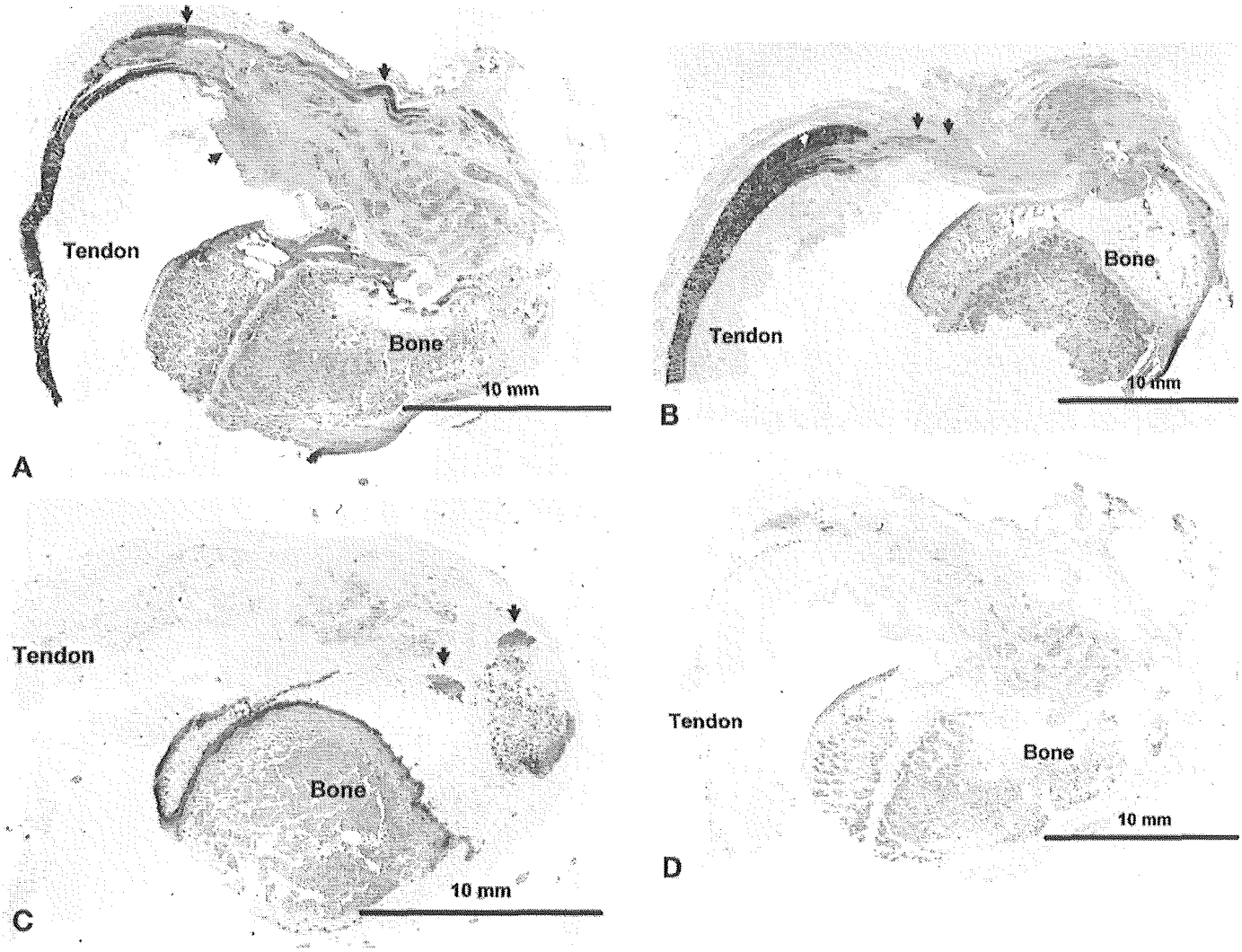

Figure 6. Micrographs of each group 12 weeks after surgery. A, type I collagen staining in the cell-seeded scaffold group (type I collagen stain). Note that the regenerated tendons treated with the cell-seeded scaffold were positive for type I collagen (black arrows). B, type I collagen staining in the non-cell-seeded scaffold group. Note the absence of staining (black arrows). C, type II collagen staining in the cell-seeded scaffold group. Note the presence of type II collagen in the tendon-bone insertion (black arrows). D, type III collagen staining in the cell-seeded scaffold group. Immunostaining for type III collagen was not clearly detected when compared with type I collagen (B).

ferences in cell numbers or collagen formation between the CSS and NCSS groups (Figures 3 A-C). Many fibroblasts and macrophages were observed around the scaffold fibers in both groups (Figures 3 B and C). In the control group, there was a thin membrane with a number of fibroblasts and vessels (Figure 3D). The hybrid fiber scaffold remained in the regenerated tissues in all sections. No rupture of the scaffold or severe inflammatory response was observed microscopically in any specimen. All sections were immunohistochemically negative for types I, II, and III collagen at this time.

12-Week Specimens. In both the CSS and NCSS groups, the created defect was covered macroscopically with thick fibrous tissues. There appeared to be continuity between the infraspinatus muscle and its bone insertions (Figure 4). In the control group, although the defects were not covered with any tissues at 4 weeks, at 12 weeks the defects were covered with thin fibrous membranes. Microscopically, the number of fibroblasts in both the CSS and NCSS groups did not increase significantly from 4 to 12 weeks postoperatively (Figures 5 A and B). The characteristic crimp patterns in the CSS group were more regularly arranged than were those in the NCSS group (Figures 5 A and B). The hybrid fiber scaffold was more extensively absorbed at 12 weeks than at 4 weeks. In the control group, thin membranes with fibroblasts linked the end of the torn cuff to the bone (Figure 5C). Immunohistochemistry at this point showed positive staining for type I collagen on the periphery of the

TABLE 1
Mechanical Properties of the Regenerated Tissues

	Cross-sectional Area, mm^2	Tensile Strength, MPa	Tangent Modulus, MPa
12-week control[a]	3.7 ± 0.5	5.5 ± 0.8	37.4 ± 5.4
Cell-seeded scaffold group			
4 wk	8.5 ± 1.0	4.8 ± 0.8	54.7 ± 5.7
12 wk	10.3 ± 1.2[b]	9.2 ± 0.8[c,d]	89.0 ± 7.4[c,e,f]
Non-cell-seeded scaffold group			
4 wk	8.2 ± 1.0	5.3 ± 1.6	59.1 ± 7.2
12 wk	9.9 ± 1.3[b]	7.1 ± 0.8	60.2 ± 6.5[g]

[a]Control, defect was left uncovered. The defect in the rotator cuff was not covered with any regenerating tissues in the control group at 4 weeks.
[b]$P < .001$ versus 12-week control.
[c]$P < .01$ versus 4-week cell-seeded scaffold group.
[d]$P < .01$ versus 12-week control.
[e]$P < .01$ versus 12-week non-cell-seeded scaffold group.
[f]$P < .0001$ versus 12-week control.
[g]$P < .05$ versus 12-week control (n = 6, mean ± SE).

implanted scaffold in the CSS group (Figure 6A), whereas there was no type I collagen staining in the NCSS group (Figure 6B). Type II collagen was observed in the tendon-bone insertion in half of the specimens in each group (Figure 6C). Immunostaining for type III collagen was not clearly detected in the CSS group in comparison with type I collagen (Figure 6D).

Mechanical Properties of Regenerated Tissue

Before testing the mechanical properties of the regenerated tissues, we evaluated the tensile strength and tangent modulus of intact infraspinatus tendons; the respective values were 54.5 ± 13.1 MPa and 582.5 ± 93.2 MPa.

All rotator cuff–humerus complexes failed at the mid-substance of the regenerated tissue portion except for the 4-week control specimens. Table 1 summarizes the results of the analysis. In the CSS group, both tensile strength and tangent modulus increased significantly to 191% and 163%, respectively, from 4 to 12 weeks after surgery ($P < .01$). In the NCSS group, the tensile strength and tangent modulus showed no significant alterations over the same period ($P = .11$ and .91, respectively). There were no significant differences in the cross-sectional area between the CSS and NCSS groups at 4 and 12 weeks after surgery. On the other hand, at this point, the cross-sectional areas in both groups were significantly greater than those of the control group ($P < .001$). Although there were no significant differences in the tensile strength and the tangent modulus at 4 weeks among the 3 groups, the tangent modulus at 12 weeks in the CSS group was significantly greater than in the NCSS and control groups ($P < .01$ vs the NCSS group; $P < .0001$ vs the control group).

DISCUSSION

The limited healing potential of the rotator cuff requires intensive reconstructive procedures to treat massive tears. However, each procedure has considerable limitations, as mentioned previously. The ideal treatment for irreparable tears would be to regenerate the tendon tissue, which mainly consists of type I collagen. In this study, we hypothesized that the enhancement of type I collagen products in the regenerated tissue could increase the mechanical strength in a living body. To test this hypothesis, we used a rabbit rotator cuff rupture model treated with tissue engineering techniques using a novel 3D scaffold. Four to 12 weeks after surgery, immunohistochemistry showed an increase of type I collagen products in the regenerated tissue in the CSS group. Moreover, the tensile strength and tangent modulus also improved significantly. By contrast, tissues from the other experimental groups showed no significant increases in type I collagen products or improvements in mechanical properties. The NCSS group showed no increase of type I collagen products and no statistically significant improvement of the mechanical properties from 4 to 12 weeks. Although there may be a lack of statistical power in the analysis of mechanical properties, we reasonably conclude that an increase of type I collagen contents appears to enhance the mechanical strength of the regenerated tissues. This finding provides important and fundamental information for the development of a tendon and ligament tissue engineering technique.

Several tissue engineering studies have shown successful ligament and tendon regeneration using a variety of scaffold materials, including both natural and synthetic materials.[1,4,7-9,12] However, little attention has been given to whether these scaffold materials can mechanically support the transplanted fibroblasts and the regenerated tissues in a living body. Frank et al showed that recovery of the material properties of a ligament scar improved up to 14 weeks, but the maximum stress or strain remained lower up to 40 weeks of healing compared with a normal ligament.[10] Although scaffold materials need to be biodegradable, they must still provide adequate mechanical strength for immature tissues during the process of ligament and tendon regeneration. In our previous study, we demonstrated that HA enhanced not only the biological effects on the seeded fibroblasts but also the mechanical strength of the polymer fiber.[11] The tensile strength of the scaffold, which was fabricated from the chitosan-based HA hybrid fibers, was 80 MPa under dry conditions. Gentleman et al reported that the tensile strength of bovine Achilles tendon collagen fibers (36 MPa) was similar to that reported for human ligament.[12] The tensile strength of this scaffold was higher than that of a collagen construct under dry conditions. Although our fiber scaffold became mechanically weaker over time, it appeared to be strong enough to maintain continuity between the infraspinatus muscles and their bone insertions until the native ECM had matured.

Regarding the application of the current technique to the treatment of irreparable rotator cuff tears, we must also consider the tendon-bone junction between the

humerus and regenerated tissue. In operations for rotator cuff tears, the distal end of the ruptured tendon is fixed directly to the humerus. Therefore, a successful technique requires the scaffold to adhere firmly to the bone. Histologically, we observed here a secure connection between the regenerated tissue and the insertion of the humerus. Several methods for augmenting the tendon-bone junction have shown enhanced healing potential. A woven polylactic acid scaffold on the tendon-bone site strengthened repairs of the rotator cuff,[15] whereas bone marrow stromal cells and osteoinductive proteins such as bone morphogenetic protein enhanced tendon-to-bone healing.[3,24] In the present study, although the regenerated tendon-bone junction was not similar to a normal cuff insertion including the tidemark, type II collagen was seen in the regenerated region. Therefore, this scaffold material may offer an advantage in reconstructing secure insertions consisting of fibrocartilage layers.

We must also consider the origin of fibroblasts embedded in the regenerated tissue. The fate of donor cells seeded on a scaffold after implantation into a host body has not been clarified. Several studies have demonstrated that the host cells gradually replace the implanted donor cells over time.[21,23] Bellincampi et al[5] showed that anterior cruciate ligament fibroblasts, which were seeded onto collagen scaffolds, remained viable for at least 4 to 6 weeks after being implanted in knee joints. Mierisch et al[21] reported that the transplanted chondrocyte density decreased to 15% of the initial density at 4 weeks after implantation into an osteochondral defect in rabbits. Ostrander et al[23] examined the fate of perichondrium cells in the repair of osteochondral defects. They showed a decline in donor cells accompanied by an influx of host cells into the repair tissue. In the current histological findings, the cells and regenerated tissue were mainly found on the superficial layer of the scaffold. Immunohistochemically, type I collagen was localized on the surface of the scaffold. On the other hand, the potential of chitosan as a biomaterial is based on its cationic nature and high-charge density in solution. Madihally and Matthew[19] reported that the cationic nature of chitosan allows for electrostatic interactions with anionic glycosaminoglycans (GAGs), proteoglycans, and other negatively charged species. These ionic interactions serve as a mechanism for retaining and recruiting cells, growth factors, and cytokines within a tissue scaffold. We therefore believe that host cells recruited from the surrounding tissue gradually replace the transplanted fibroblasts after several weeks. This theory explains the scarcity of cells in the central portion of the implanted scaffold. In addition, no expression of type I collagen was found in the acellular scaffold-implanted control group of rabbits. We postulate that the donor cells mainly contribute to tissue regeneration immediately after transplantation to the host. Further studies will be performed to confirm these points on the fate and roles of donor cells.

The GAGs, which are parts of the ECM components, play an important role in regulating the expression of the cellular phenotype and in supporting tissue regeneration. Regarding our scaffold material, it is notable that HA, which is a main component of the GAGs of the rotator cuff,[6,27] is applied to chitosan as a fundamental substance. Many studies have shown the biological effects of HA on various cells.[14,18,28,31] In tendon tissue engineering, we must consider that the tendon is subject to excessive mechanical stress. To maintain the attached fibroblasts under this circumstance, highly cellular adhesiveness is a requirement for scaffold materials. Zimmerman et al[31] showed that HA is an adhesion modulator molecule that can mediate the early stage of cell-substrate interaction. Hu et al[14] stated that HA has positive advantages for fibroblast adhesion. Based on those data, it seems reasonable to conclude that scaffold biomaterials introducing HA will provide excellent fibroblast adhesive activity. The high adhesiveness of this scaffold material could enhance tissue regeneration in vivo.

There were several limitations to this study. First, the biodegradability and biocompatibility of the scaffold material remain unclear. Although chitosan has been employed as an excellent biocompatible material for wound healing and tissue repair, immunological reactions have been reported. Here, we found no significant inflammation with mononuclear cell infiltrates around the implanted scaffold. However, further observation must be made to confirm the long-term general or local immune reaction. Second, as mentioned above, the regenerated tissue, mainly consisting of type I collagen, was localized in the superficial layer of the scaffold. This phenomenon has been considered to be caused by central necrosis in 3D culture systems. To increase the mechanical strength of regenerated tissue, the tissue must be distributed throughout the entire scaffold. It is therefore necessary to improve the culture environment so as to spread both nutritive and soluble cell growth factors. In addition, the pore size of the scaffold strongly affects fibroblast invasion and angiogenesis into the 3D scaffold. We aim to design a better scaffold material with adequate porosity for these purposes. Finally, the data obtained demonstrated that the mechanical properties of tissues regenerated from the CSS only approximated 20% of those of the intact infraspinatus tendon at 12 weeks postoperatively. Histologic findings show that the scaffold material still remained in the regenerated tissues at 12 weeks postoperatively. Therefore, to improve the mechanical properties of the regenerated tissues, the mechanical strength of the current scaffold material must be increased. For application in the treatment of human rotator cuff tears, these structural and mechanical assessments will be performed to progress from success in our small-animal model to trials with full-size defects in a large-animal model.

In conclusion, this study confirmed that a 3D scaffold constructed from chitosan-based HA hybrid polymer fibers enhanced the production of type I collagen and provided sufficient mechanical strength for the regenerated tissue of the rotator cuff in vivo. Although there were several limitations, these results strongly suggest the feasibility of rotator cuff regeneration using current tissue engineering techniques with this novel 3D scaffold.